



Economic analysis of vanillin production from Kraft lignin using alkaline oxidation and regeneration

Thang Toan Vu^{1,2} · Young-Il Lim¹ · Daesung Song² · Kyung-Ran Hwang³ · Deog-Keun Kim³

Received: 3 October 2020 / Revised: 12 December 2020 / Accepted: 14 December 2020 / Published online: 4 January 2021
© The Author(s), under exclusive licence to Springer-Verlag GmbH, DE part of Springer Nature 2021

Abstract

Lignin conversion to vanillin is one of the promising routes for lignin valorization. This study presents an economic analysis for the conceptual design of vanillin production from 10 t/h Kraft lignin. The vanillin plant includes alkaline oxidation of lignin with NaOH, ultrafiltration, chromatographic separation, and crystallization to purify vanillin. A boiler for the combustion of waste lignin was used to supply steam required for oxidation reactions and water evaporation. Sodium carbonate (Na₂CO₃) formed in the combustor was regenerated into NaOH using lime. The heat network was integrated to reduce the consumption of cooling water, steam, and electricity. The plant produced 0.52 t/h vanillin with a yield of 5.2%. The return on investment (ROI) and payback period of this plant were 10.1%/year and 8.0 years, respectively. The ROI was most sensitive to the vanillin price. The desired ROI of 15%/year can be achieved with a plant size of 20 t/h lignin.

Keywords Kraft lignin · Vanillin · Alkaline oxidation · Alkali regeneration · Economic analysis · Heat integration

1 Introduction

Lignin is one of the most abundant aromatic substances in woody materials, agricultural residues, and other plant materials, representing approximately 25% of the available biomass [1, 2]. The main source of lignin is black liquor from

the pulp and paper industry, where the Kraft process accounts for almost 80% of chemical pulp production [3, 4]. Even though around 60 million tons of lignin was extracted in 2015 [5], only a small amount of lignin was used as raw material for the production of added-value chemicals [6, 7]. The most lignin is generally burnt at the factory as a fuel [7–9]. The insufficient usage of lignin is mainly caused by its recalcitrant nature and heterogeneous structure [2]. Lignin is a biopolymer, which mainly consists of methoxylated phenylpropane structures and can potentially be used as a raw material for high-value chemicals [7, 10]. Among these chemicals, vanillin (C₈H₈O₃) as a mono-aromatic compound is a good candidate because it is widely used in the food, cosmetic, and pharmaceutical industries [11]. In addition, vanillin is one of the most widely produced aroma chemicals as it is a non-toxic aromatic with reactive functional groups that can be chemically modified [12].

Three major approaches have been developed for vanillin synthesis: oxidation of eugenol, oxidation of liginosulfonates, and the contemporary technique utilizing guaiacol and glyoxylic acid based on petrochemical routes [13]. The oxidation of eugenol is not commercially applied, whereas the glyoxylic technique currently dominates the market [5]. Liginosulfonate fractions from the sulfite pulping process are oxidized in order to depolymerize lignin and produce vanillin in an alkaline environment at high temperature under high

✉ Young-Il Lim
limyi@hknu.ac.kr

✉ Daesung Song
dssong@jnu.ac.kr

Thang Toan Vu
toanthangbk95@gmail.com

Kyung-Ran Hwang
hkran@kier.re.kr

Deog-Keun Kim
dkkim@kier.re.kr

¹ CoSPE, Department of Chemical Engineering, Hankyong National University, 327 Jungang-ro, Anseong 17579, Republic of Korea

² School of Chemical Engineering, Chonnam National University, 77 Yongbong-ro, Buk-gu, Gwangju 61186, Republic of Korea

³ Future Energy Plant (FEP) Convergence Research Center, Korea Institute of Energy Research, Gajeong-ro 152, Yuseong-gu, Daejeon 34129, Republic of Korea

pressure [8, 14]. The commercial process for vanillin production from lignosulfonates includes alkaline oxidation, solvent extraction, distillation, and crystallization [8]. However, the lignin-based vanillin production is not widely available because of the intensive purification process [15] and low production yield [16].

Under alkaline condition, lignin is ionized, oxidized, and depolymerized by oxygen to aromatic aldehydes such as vanillin and organic acids such as formic acid [1, 17]. In most studies, vanillin was produced from lignin solution, where sulfite liquor served as the raw material, leading to a higher yield of vanillin by direct oxidation (15 wt%) than achieved from Kraft lignin (12 wt%) [18]. However, because Kraft lignin (brown powder) accounts for the majority of lignin extracted from the chemical pulping process [8], oxidation of Kraft lignin has been studied for producing high value-added compounds [7]. Mathias et al. oxidized Kraft lignin in an alkaline medium comprising 2 M NaOH [19]. Alkaline oxidation of Kraft lignin was performed to produce vanillin in a bubble column reactor with structured-packing, affording high O₂ mass transfer [11]. Silva et al. [20] proposed an integrated process including oxidation of Kraft lignin in alkaline medium, vanillin recovery with ultrafiltration and ion-exchange chromatography, and synthesis of polyurethane. Araújo et al. proposed a mathematical model for the oxidation of Kraft lignin in a batch reactor [21]. Vanillin with a yield of 6.5% was produced from Kraft lignin via alkaline oxidation in the presence of a Cu-Mn mixed oxide catalyst [22]. A high vanillin yield of 10.9% was reported combining solvent fractionation and CuSO₄ catalyzed oxidation of Kraft lignin [7]. A sequence involving alkaline oxidation, filtration, chromatographic separation, and crystallization was proposed for the recovery of vanillin from Kraft lignin [23, 24]. Gomes and Rodrigues [15] obtained vanillin with a purity of 96% by a lab-scale experiment with an alkaline oxidation of Kraft lignin, ultra- and nano-filtrations, adsorption, extraction by ethyl acetate, and crystallization.

Besides alkaline oxidation of Kraft lignin, several studies suggested acidic lignin oxidation processes. Partenheimer successfully isolated a number of expected products, including vanillin and syringaldehyde, from various lignins by using metal/bromide catalysts in acetic acid [25]. A promising amount of vanillin (7 wt% yield) was extracted from Indulin AT Kraft lignin in methanol/water solvent [26], where lignin was oxidized with O₂ at 10 bar. Werhan et al. performed acidic oxidation of Kraft lignin in a batch reactor, as well as a continuous two-phase micro-reactor [27]. Nevertheless, the acidic oxidation of lignin is in the early stage of development [2].

Efficient lignin conversion into desired aromatics is an essential topic in the current biorefinery research [9]. Technological advances in Kraft lignin-based vanillin production were reported, making lignin-based vanillin plants

economically viable. Zabkova et al. recommended a downstream process using ultrafiltration and ion-exchange for the recovery of vanillin from a lignin/vanillin mixture [28]. Wongtanyawat et al. compared several separation technologies for a vanillin plant with acidic oxidation of Kraft lignin in terms of energy consumption and life cycle analysis, where vanillin separation via adsorption on a zeolite was the best alternative because the solvent recovery system for extraction was not needed [4]. Khwanjaisakun et al. investigated the internal rate of return (IRR) of Kraft lignin-based and petroleum-based vanillin production, and showed that the lignin-based vanillin plant with solvent extraction using ethyl acetate was compatible with the petroleum-based plant [16]. Unfortunately, the solvent extraction processes require a large amount of solvent and a solvent recovery unit. Even though the combination of ultrafiltration and chromatographic separation is expected to be a good candidate for solvent-free vanillin separation, economic feasibility analysis of the solvent-free vanillin process has never been presented. Moreover, previous studies focused exclusively on vanillin production without considering alkali regeneration and wastewater treatment.

In this work, economic analysis of a conceptual Kraft lignin-based vanillin plant is undertaken. Based on the similarity between alkaline lignin oxidation and Kraft pulping, the alkali regeneration process is integrated with the vanillin plant in order to recover alkali (NaOH). The process consists of alkaline aerobic oxidation of lignin, solvent-free vanillin separation and purification, combustion of waste lignin in a steam boiler, NaOH regeneration, and wastewater treatment. The process performance with heat integration is evaluated in terms of the vanillin production yield and energy consumption. The economic parameters, such as the total capital investment (TCI), total production cost (TPC), return on investment (ROI), and payback period (PBP), are estimated. This study provides a useful tool for assessing the technical and economic value of the lignin-to-vanillin process.

2 Process description and design

Indulin AT Kraft lignin with a moisture content of 4.5% was used as the feedstock in this study. The results of proximate and ultimate analyses are shown in Table 1 [29]. The lower heating value (LHV) of lignin, calculated by using the Boie formula [30], was 25.2 MJ/kg.

The vanillin plant for processing Kraft lignin included eight areas: alkaline aerobic oxidation of lignin (A100), ultrafiltration (UF) and chromatographic separation for solvent-free vanillin recovery (A200), crystallization of vanillin (A300), waste lignin combustion (A400), low-pressure (LP) and medium-pressure (MP) steam generation (A500), alkali regeneration (A600), wastewater treatment (WWT) and utilities

Table 1 Proximate and ultimate analyses of the Kraft lignin used in this study [29]

Proximate analysis (wt%)	Moisture	4.5
	Volatile matter	60.0
	Fixed carbon	32.2
	Ash	3.3
	Total	100
Ultimate analysis (wt%, dry basis)	C	63.9
	H	5.8
	O	24.6
	N	0.7
	S	1.5
	Ash	3.5
	Total	100

for cooling water, refrigeration, and steam (A700), and natural gas (NG) combustion (A800), as shown in Fig. 1.

2.1 Operating conditions and process performance

The operating conditions and process performance are summarized in Table 2 for the main equipment in each area. The alkaline oxidation reactor in A100 is a key piece of equipment for producing vanillin from Kraft lignin. A structured-packing bubble column reactor was used for the lignin oxidation. Sixty percent lignin with O₂ was oxidized over a copper-based catalyst and depolymerized at 160 °C and 10 bar in 7.4% NaOH solution; 40% lignin was left in the solid phase [21]. The converted lignin (60%) in the liquid phase was modeled by vanillin (C₈H₈O₃), syringaldehyde (C₉H₁₀O₄), vanillic acid (C₈H₈O₄), acetovanillone (C₉H₁₀O₃), acetic acid (C₂H₄O₂), formic acid (CH₂O₂), lactic acid (C₃H₆O₃), and *p*-hydroxybenzaldehyde (C₇H₆O₂) with an inlet lignin-based yield of 6, 0.5, 3, 1, 20, 10, 10, and 9.5%, respectively, which was inspired by the work of Jeon et al. [22] and Lyu et al. [17]. All organic compounds except for recovered vanillin were

assumed to be treated in the wastewater treatment area (A700). The two different vanillin forms were defined as vanillin-1 (liquid) and vanillin-2 (crystal). The residence time was assumed to be 40 min [21].

The vanillin separation efficiency using ultrafiltration and chromatographic separation was assumed to be 95% [31] and 96.2% [32], respectively. Vanillin with 99.5% purity and 94.3% yield [16] was produced in a crystallizer. Thus, the overall recovery of vanillin based on the inlet Kraft lignin was 5.18%, which is lower than that (8.2%) reported by Wongtanyawat et al. [4] and higher than that (4.3%) obtained by Gomes and Rodrigues [23].

The alkaline oxidation reactor in A100 operating at 160 °C and 10 bar was heated by MP steam. Three evaporators operating at 100 °C and 1 bar were present in A300 (crystallization), A400 (lignin combustion), and A700 (WWT) to remove water from the vanillin solution, wet waste lignin, and NaOH solution, respectively. The permeate stream exiting ultrafiltration was subjected to strong cation exchange chromatography to recover vanillin [32]. The vanillin mixture was crystallized at 5 °C, where the solubility of vanillin in water was obtained from the literature [33].

The waste lignin as the retentate from ultrafiltration was concentrated in a three-stage multi-effect evaporator [34] in A400 (see Fig. S5 in the Supplementary Material). The waste lignin combustor equipped with an electrostatic precipitator (ESP) was operated at 850 °C, with a carbon conversion of 99% [34]. One hundred percent NaOH left in the lignin residue formed Na₂CO₃ with CO₂ in the combustor. N₂ from primary and secondary air and lignin decomposition formed NO with a conversion of 0.1%. Ninety-nine percent sulfur in lignin was converted to SO₂, emitting approximately 1000 ppm SO₂. During flue gas desulfurization, the flue gas was cooled with limewater, and 92% SO₂ was removed. The flue gas from the lignin combustor (A400) and NG combustor (A800) exited through the stack, where the SO₂ concentration was 9 ppm satisfying the regulation limit (under 25 ppm) [35].

The steam boiler in A500 produced LP steam at 2.3 bar and MP steam at 8.7 bar using the heat obtained from the waste lignin combustor in A400 and NG combustor in A800. The NG was composed of 94.7% CH₄, 2.1% C₂H₆, 0.4% C₃H₈, 0.2% C₄H₁₀, 1.0% CO₂, and 1.6% N₂. The MP steam was used to heat the alkaline oxidation reactor (A100), while the LP steam was supplied to the three evaporators. The alkali regeneration process in A600 included the recausticizing reactor, water scrubber, filter, and calcination reactor. Na₂CO₃ (molten smelt) separated in A400 was recausticized at 90 °C into NaOH with Ca(OH)₂ [36]. CaCO₃ was calcined at 1100 °C to form CaO [37], where NG was used for heating.

The cold and hot energy streams such as cooling water and steam were collected and distributed in the utility area (A700). All organic compounds soluble in the wastewater were digested in the aerobic bioreactor in A700 to give water and

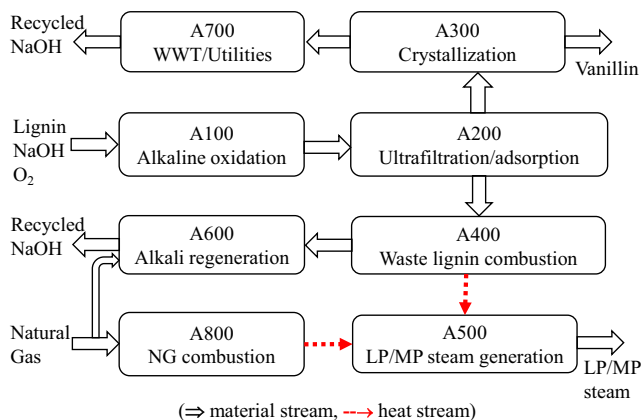
**Fig. 1** Conceptual design for vanillin production from Kraft lignin

Table 2 Operating conditions and performance of main reaction and separation processes

Area	Equipment	Operating condition	Performance	Reference
A100	Alkaline oxidation reactor	$T = 160\text{ }^{\circ}\text{C}$ $P = 10\text{ bar}$ Residence time = 40 min 7.4 wt% NaOH solution	Lignin conversion = 60% Vanillin yield = 6.0%	Araujo et al., 2010
A200	Ultrafiltration	$T = 25\text{ }^{\circ}\text{C}$ $P = 41\text{ bar}$	η^a of liquid = 95%	Arkell et al., 2014
	Chromatographic separation	$T = 25\text{ }^{\circ}\text{C}$ $P = 1\text{ bar}$	η of vanillin = 96.2%	Gomes and Rodrigues, 2019
A300	Evaporator 1	$T = 100\text{ }^{\circ}\text{C}$ $P = 1\text{ bar}$	η of water = 98%	
	Crystallizer	$T = 5\text{ }^{\circ}\text{C}$ $P = 1\text{ bar}$	Crystallization yield = 94.3% Vanillin purity = 99.5%	Khwanjaisakun et al., 2020
A400	Evaporator 2	$T = 100\text{ }^{\circ}\text{C}$ $P = 1\text{ bar}$	η of water = 98%	
	Waste lignin combustor	$T = 850\text{ }^{\circ}\text{C}$ $P = 1.04\text{ bar}$	Carbon conversion = 99% NaOH conversion = 100% NO conversion = 0.1% SO ₂ conversion = 99%	Humbird et al., 2011
	Flue gas desulfurization	$T = 56\text{ }^{\circ}\text{C}$ $P = 1\text{ bar}$	SO ₂ removal efficiency = 92%	
A500	Steam boiler	LP steam: $T = 125\text{ }^{\circ}\text{C}$ $P = 2.3\text{ bar}$	MP steam: $T = 175\text{ }^{\circ}\text{C}$ $P = 8.7\text{ bar}$	Humbird et al., 2011
A600	Alkali regeneration	$T = 90\text{ }^{\circ}\text{C}$ $P = 1\text{ bar}$	Na ₂ CO ₃ conversion = 80%	Sanchez, 2007
	Filtration of solid	$T = 25.4\text{ }^{\circ}\text{C}$ $P = 5\text{ bar}$	η of solid = 96% Water in solid = 20%	Sanchez, 2007
	Calcination	$T = 1100\text{ }^{\circ}\text{C}$ $P = 1\text{ bar}$	CaCO ₃ conversion = 100%	Lundqvist, 2009
A700	Evaporator 3	$T = 100\text{ }^{\circ}\text{C}$ $P = 1\text{ bar}$	η of water = 98%	
	Aerobic bioreactor	$T = 25\text{ }^{\circ}\text{C}$ $P = 1\text{ bar}$	Aerobic reaction conversion: 100%	Humbird et al., 2011
	Cooling water tower	$T_{\text{out}} = 28\text{ }^{\circ}\text{C}$ $T_{\text{in}} = 37\text{ }^{\circ}\text{C}$	Cooling water loss = 1.5%	
A800	Natural gas combustor	$T = 812\text{ }^{\circ}\text{C}$ $P = 1.1\text{ bar}$	Carbon conversion = 100%	

^a η : separation efficiency (= $100 \times \text{outlet mass}/\text{inlet mass}$)

CO₂ [34]. The cooling water was supplied at 28 °C and returned at 37 °C throughout the facility. A total of 1.5% cooling water was lost in the cooling water tower. A refrigerator with ammonia as a refrigerant was used for the crystallization system operating at 5 °C [38].

Figure 1 shows the basic design flowsheet with heat integration inside each area. Heat integration between areas is required to reduce the energy consumed for the cooling water, steam, and electricity.

2.2 Heat exchange networks

In high energy consumption plants, the integration of a heat exchange network for the cold and hot streams is needed to save the operating cost by reducing the cold and hot utilities [39–41]. The pinch point is a location in the heat exchange

network where the temperature difference (ΔT_{min}) between the cold and hot streams is minimum. The higher the ΔT_{min} , the more utility is required. However, a lower ΔT_{min} requires larger and more costly heat exchangers. The optimal value of ΔT_{min} is commonly 15–20 °C [42]. In this study, ΔT_{min} was set to 20 °C.

Four heat integration streams with additional heat exchangers were employed in the vanillin plant, as shown in Fig. 2. The hot product stream at 161 °C and 41 bar before entering ultrafiltration must be cooled to 25 °C in A200. Before entering the crystallizer, water has to be removed from the liquid product and evaporation heat is needed in A300, which is heated by LP steam. Two more evaporators are present in A400 and A700, as mentioned earlier. The heat exchange networks between A100, A200, A300, A400, and A700 are integrated and the energy consumption is reduced.

2.3 Process flow diagram with heat integration

The process flow diagram (PFD) for the vanillin plant with heat integration was constructed using a commercial process simulator (ASPEN Plus, ASPEN Tech, USA) to calculate the mass and energy balances. The alkaline oxidation reactor in A100 was modeled by a yield reactor (RYield), whereas the reactors such as the waste lignin combustor in A400, recausticizing and calcination reactors in A600, aerobic bioreactor in A700, and NG combustor in A800 were formulated as stoichiometric reactors (RStoic) with a given conversion. All separation equipment such as the ultrafiltration, chromatographic separation, crystallization, and solid filter systems were modeled by a simple separator with a given separation efficiency that was obtained from the literature (see Table 2). Figure 3 presents the PFD focused on heat integration between areas. The heat integration streams between A100–A200, A200–A400, A200–A300, and A200–A700 are represented by HI1–HI2, HI3–HI4, HI7–HI8, and HI5–HI6, respectively. Four heat exchangers satisfying ΔT_{\min} for the heat integration are shown in Fig. S1 (A100), Fig. S4 (A300), Fig. S5 (A400), and Fig. S9 (A700) in the Supplementary Material. The detailed PFDs for the eight areas (A100–A800) are presented in S1 (flowsheets) in the Supplementary Material. The temperature (T), pressure (P), mass flow rates (F), enthalpy flow rates (H), compositions (x_i), heat duty (Q), and work (W) are indicated in S2 (stream tables) in the Supplementary Material.

Since the process includes polar non-electrolyte compounds such as acetic acid, the non-random two-liquid Hayden–O’Connell (NRTL-HOC) thermodynamic model was chosen for A100–A400. The Peng–Robinson and Boston–Mathias (PR–BM) equation of state was selected for the remaining areas.

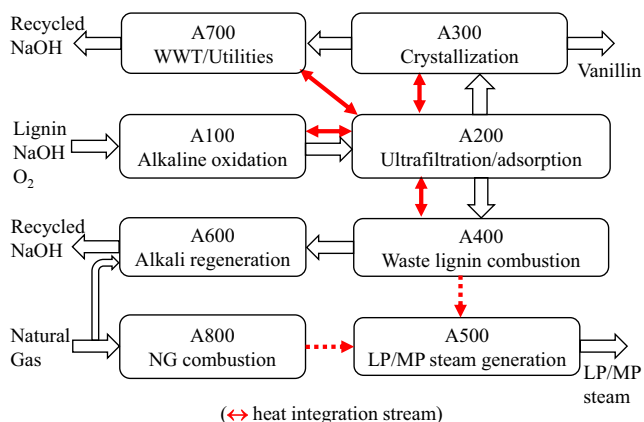


Fig. 2 Heat integration proposed in this study for vanillin production from Kraft lignin

3 Economic analysis method

Economic analysis was performed to calculate the TCI, TPC, ROI, and PBP [43, 44] under several assumptions. The sensitivity analysis was conducted to examine the effect of the fluctuation in key economic parameters on the process feasibility.

3.1 Estimation of TCI and TPC

The equipment type and size were determined based on the stream data obtained from the process simulation. The direct and indirect equipment cost (C_{DI}), including the equipment purchased cost, installation cost, and indirect cost, was calculated using the capacity ratio method [40]:

$$C_{DI} = C_{DI,ref} \cdot \left(\frac{A}{A_{ref}} \right)^{\phi} \frac{I}{I_{ref}} \quad (1)$$

where A is the capacity of the equipment; $C_{DI,ref}$ is the direct and indirect cost of the equipment with a capacity of A_{ref} ; and I and I_{ref} are the chemical engineering plant cost index (CEPCI) of the current year (2018 in this study) and the reference year, respectively. The capacity exponent (ϕ) was in the range of 0.6–1, depending on the type of equipment. The reference cost ($C_{DI,ref}$) was obtained from the NREL reports of 2011, 2015, and 2018 [34, 45, 46] and Couper et al. [47], considering 2009, 2010, 2011, 2013, 2014, and 2016 as reference years. The CEPCIs in 2009, 2010, 2011, 2013, 2014, 2016, and 2018 were 521.9, 550.8, 585.7, 567.3, 576.1, 541.7, and 603.1, respectively.

The fixed capital investment (FCI) and TCI were estimated using the factorial method [40, 44]. The FCI is the sum of all C_{DI} and project contingency, and the TCI includes the FCI and working capital.

$$FCI = (1 + c) \sum_{j=1}^N C_{DI,j} \quad (2)$$

$$TCI = (1 + d) FCI \quad (3)$$

where N is the number of equipment, c is the project contingency factor (0.1), and d is the working capital factor (0.05) [43, 44].

The TPC comprises the raw material cost (C_R), utility cost (C_U), and fixed cost (C_F):

$$TPC = C_R + C_U + C_F \quad (4)$$

C_U includes the costs of cooling water, refrigeration, NG, and electricity. C_F is the sum of the operating labor cost (C_{labor}), maintenance cost (C_{main}), operating charges (C_{oper}), plant overhead (C_{OH}), and general and administration cost

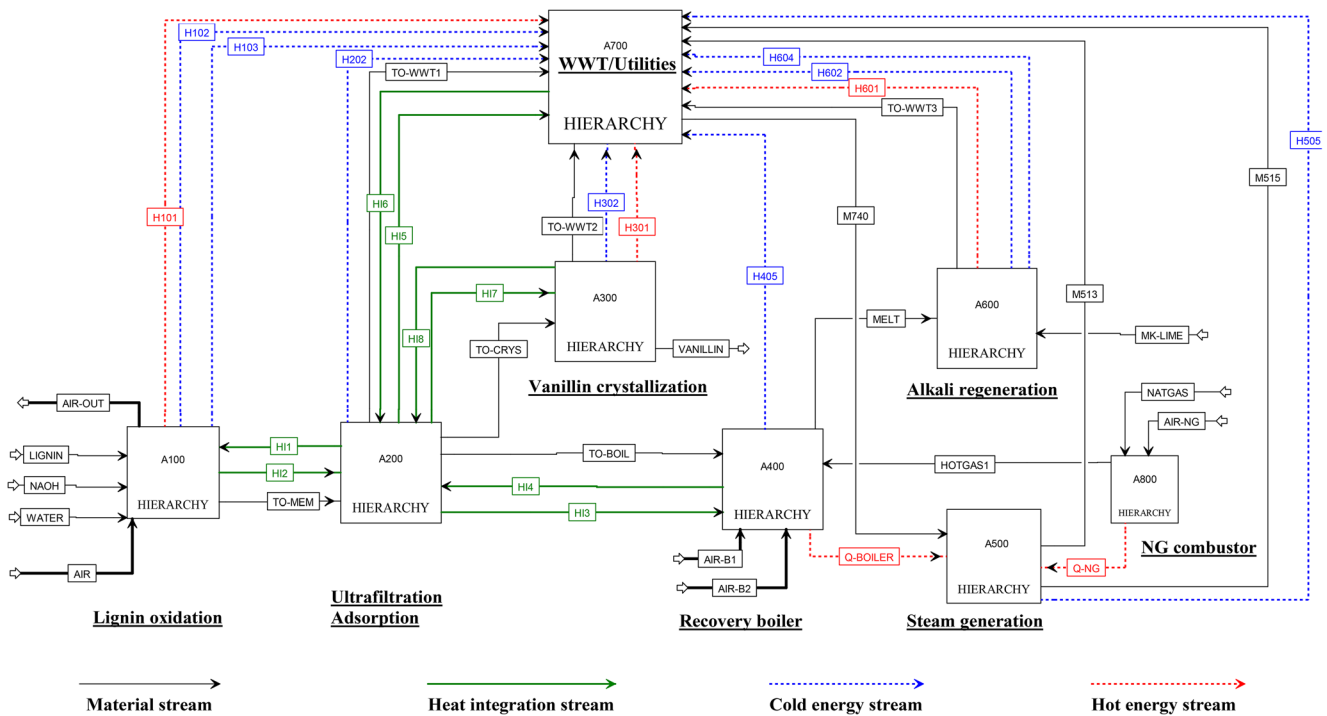


Fig. 3 Process flow diagram (PFD) of plant with heat integration for vanillin production from Kraft lignin

(C_{GA}) [40, 44].

$$C_F = C_{labor} + C_{main} + C_{oper} + C_{OH} + C_{GA} \quad (5)$$

where C_{main} is set to 7% of the FCI and C_{oper} , C_{OH} , and C_{GA} are 25%, 70%, and 8% of C_{labor} , respectively. Thus, Eq. (5) leads to

$$C_F = 0.07FCI + 2.03C_{labor} \quad (6)$$

where C_{labor} is calculated for 16 laborers and 5 supervisors with a salary of 40,000 \$/year/person and 80,000 \$/year/person, respectively [44].

3.2 Calculation of ROI and PBP

The ROI and PBP are well-known economic criteria for investment decisions [44]. The gross profit before tax ($P_{G,n}$) for each year (n) is given as

$$P_{G,n} = ASR(1 + \alpha)^{n-1} - TPC(1 + \alpha)^{n-1} - C_{dep,n} - C_{debt,n} \quad (7)$$

where ASR, C_{dep} , and C_{debt} are the annual sales revenue, depreciation cost, and debt repayment cost, respectively. ASR is the selling profit from vanillin. C_{dep} is given as an equal value of FCI divided by the plant life (L_p), while C_{debt} is repaid with fully amortized principal and interest payments during L_p [43].

The annual net profit ($P_{N,n}$) is the profit after paying the corporation income tax (β):

$$P_{N,n} = P_{G,n}(1 - \beta) \quad (8)$$

The average net profit ($P_{N,avg}$) is an average of the present value of $P_{N,n}$ over L_p with the interest rate (γ) [43].

$$P_{N,avg} = \frac{1}{L_p} \sum_{n=1}^{L_p} \left(\frac{P_{N,n}}{(1 + \gamma)^n} \right) \quad (9)$$

The ROI is defined as the percentage of $P_{N,avg}$ to the TCI:

$$ROI (\%/y) = 100 \frac{P_{N,avg}}{TCI} \quad (10)$$

The PBP is calculated by dividing the FCI by the present value of the annual cash flow (CF_n) averaged for L_p [40, 44]:

$$PBP = \frac{FCI}{\frac{1}{L_p} \sum_{n=1}^{L_p} \left(\frac{CF_n}{(1 + \gamma)^n} \right)} \quad (11)$$

CF_n is given as follows:

$$CF_n = P_{N,n} + C_{dep,n} - C_{cap,n} \quad (12)$$

where the annual capital expenditure ($C_{cap,n}$) was assumed to be 30% of the FCI divided by L_p , which corresponds to 30% equity [44].

3.3 Economic assumptions

Table 3 shows the economic assumptions used in this study. The plants were constructed with 30% equity, resulting in a debt ratio (λ) of 0.7. The working time (H_p) was given as 8000 h per year. The plant life (L_p) was 20 years. The startup

period was 4 months in the first year. α , β , and γ were 2%/year, 20%, and 6%/year, respectively.

The costs of cooling water, electricity, and NG were set to 0.066 \$/m³, 0.099 \$/kWh, and 10.4 \$/GJ, respectively. The operating cost for refrigeration was assumed as 20% of the refrigerator equipment cost [38]. The prices of Kraft lignin and vanillin were 260 \$/t [5] and 20 k\$/t, respectively. Since the price changes with time and location [5, 35], the prices of Kraft lignin and vanillin have a range of 180–340 \$/t and 14–26 k\$/t, respectively, to consider their uncertainty in Section 4.3. The raw material costs and product prices reflect the market values in 2018 [45].

4 Results and discussion

The energy consumption before and after heat integration was compared for the vanillin plant. The economic parameters such as the TCI, TPC, ROI, and PBP were evaluated. Sensitivity analyses were performed for the major economic factors such as the lignin and vanillin prices, TCI, and TPC. The effect of the plant size on the ROI and PBP was determined to identify the plant size providing the desired ROI of 15%/year.

4.1 Energy consumption of vanillin plant

Table 4 compares the utility consumption before and after heat integration. Before entering ultrafiltration, one part of the hot product stream in A200 (HI1 in Fig. 3) is used to increase the temperature of the feed stream in A100 and is returned to

Table 3 Assumptions for economic analysis

Economic parameters	Value
Debt ratio (λ)	0.7
Plant availability (H_p)	8000 h/year
Plant life (L_p)	20 years
Startup time (50% plant performance)	4 months
Inflation rate (α)	2.0%/year
Corporation tax rate (β)	20%
Interest rate (γ)	6.0%/year
Price of utilities, raw materials, and products	Value
Electricity	0.099 \$/kWh
NG heating price	10.4 \$/GJ
Cooling water	0.066 \$/m ³
CaO	109.7 \$/t
Kraft lignin	260 \$/t (180–340 \$/t)
Vanillin	20 k\$/t (14–26 k\$/t)
NaOH(s)	235 \$/t
Ca(OH) ₂	262 \$/t

Table 4 Consumption of utilities before and after heat integration

Utilities	Heat integration		Utility reduction (%) ^a
	Before	After	
Cooling water (m ³ /h)	298	240	19
NG (GW _{th})	520	353	32
Electricity (MW _e)	4.4	4.0	9

^aUtility reduction (%) = 100 × (utility amount before HI – utility amount after HI)/(utility amount before HI)

A200 in stream HI2 (see Fig. 3). The pair of HI3 and HI4 is used to increase the temperature of the stream before entering the evaporator in A400. The two pairs (HI5-HI6 and HI7-HI8 in Fig. 3) conserve the thermal heat required for the evaporation of water in A700 and A300, respectively. The four pairs of heat integration allow conservation of 167 GW_{th} of NG, which corresponds to a 32% reduction in the NG utilization (see Table 4). Consequently, the amount of cooling water is reduced from 298 to 240 m³/h and the electricity for pumping the cooling water also decreases by 9%.

4.2 Analysis of economic parameters

The TEA aims to estimate the economic feasibility of the conceptual design. A breakdown of the TCI for the vanillin plant after heat integration is presented in Table 5. The equipment type and size in each area are presented in detail in S3 (main equipment and TCI) in the Supplementary Material. The purchased equipment cost (PEC) and direct and indirect equipment cost (DIC) are also reported in S3. The total direct and indirect equipment cost (C_{DI}) is \$62.2 million, where A400 (lignin

Table 5 Breakdown of total capital investment (TCI) for vanillin production from Kraft lignin in 10 t/h plant

Area	Cost (M\$ in 2018)	Percentage (%)
Alkaline oxidation (A100)	2.3	3.8
Ultrafiltration and adsorption (A200)	2.9	4.6
Crystallization (A300)	4.0	6.4
Waste lignin combustion (A400)	22.2	35.6
LP/MP steam generation (A500)	0.9	1.4
Alkali regeneration (A600)	0.3	0.4
Wastewater treatment and utility (A700)	11.7	18.9
NG combustion (A800)	12.3	19.8
Other costs (site and warehouse)	5.7	9.1
Total direct and indirect cost (C_{DI})	62.2	100
Fixed capital investment (FCI)	68.5	
Total capital investment (TCI)	71.9	

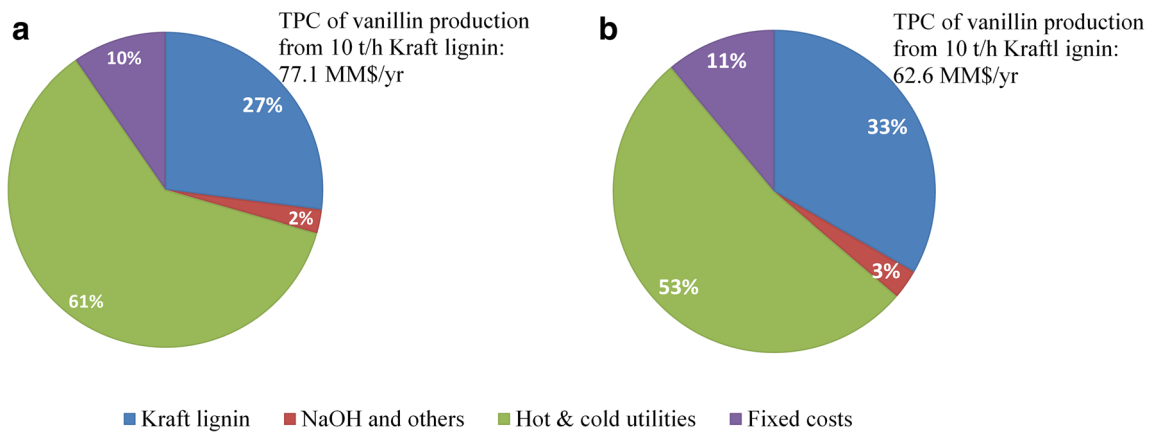


Fig. 4 Breakdown of total production cost (TPC) for vanillin production from Kraft lignin in 10 t/h plant. **a** Before heat integration. **b** After heat integration

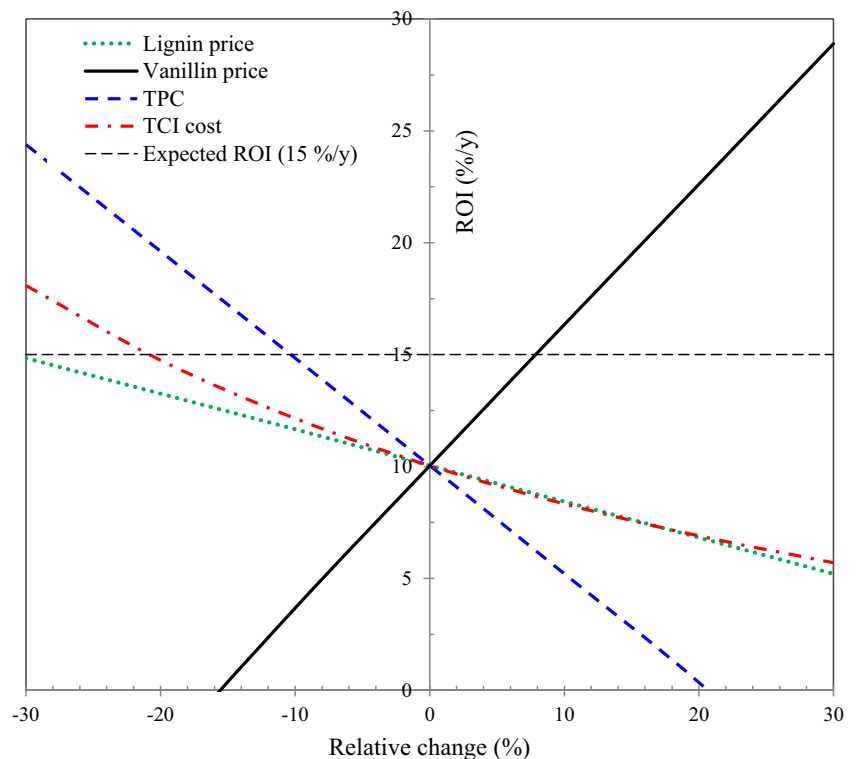
combustion and boiler area) and A800 (NG combustion area) account for 35.6% and 19.8%, respectively, representing over 50% of the C_{DI} . The FCI (Eq. (2)) sums the C_{DI} and project contingency (10% of C_{DI}). The TCI (Eq. (3)), including the FCI and working capital (5% of FCI), is \$71.9 million.

Figure 4 presents the breakdown of the TPC for the vanillin plant before and after heat integration. After heat integration, the TPC of the vanillin plant was reduced from 77.1 to 62.6 M\$/year due to the lower utility cost. The utility cost comprises the highest portion of the TPC in both cases. The cost of lignin is 20.8 M\$/year, which is 33% of the TPC for the plant after heat integration (see Fig. 4b). The fixed cost

(6.9 M\$/year), including salaries (1.0 M\$/year), maintenance cost (4.8 M\$/year), operating charges (0.3 M\$/year), plant overhaul (0.1 M\$/year), and administration cost (0.7 M\$/year), is 11% for the plant after heat integration.

The ASR averaged over the L_p is 102.6 M\$/year for the vanillin plant after heat integration. The ROI and PBP are 10.1%/year and 8.0 years, respectively. The PBP was 6.2 years for the Kraft lignin-based vanillin production with solvent extraction followed by distillation [16], which is more optimistic than that of this study. The acceptable ROI of greater than 10%/year with a PBP of less than 5 years is commonly chosen as a target in bioenergy production [48, 49]. Thus, the

Fig. 5 Plot of sensitivity of ROI to economic parameters such as lignin and vanillin prices, TCI, and TPC



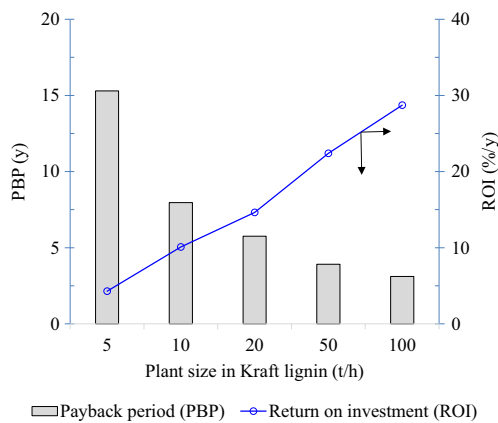


Fig. 6 Effect of plant size (5, 10, 20, 50, and 100 t/h Kraft lignin) on ROI and PBP

vanillin plant with 10 t/h lignin is not economically feasible as the PBP is unacceptable. The economic conditions providing an acceptable ROI and PBP are identified in the next section from sensitivity analysis.

4.3 Sensitivity analysis

Sensitivity analysis of the effect of the economic parameters on the ROI with $\pm 30\%$ variation is shown in Fig. 5. The effect of the vanillin price on the ROI is opposite to that of the lignin price, TCI, and TPC. The desired ROI (15%/year) is indicated by a horizontal line. The greater the slope of the ROI, the greater the influence of a given parameter on the ROI [44]. The most influential factor affecting the ROI is the vanillin price, where a 10% price increase (from 20 to 22 \$/kg) increases the ROI to 16%/year. The TPC has a greater influence on the ROI than the TCI, which suggests that the vanillin plant is production cost intensive rather than capital cost intensive. The 15%/year ROI can be achieved by reducing the TPC from 63 to 56 M\$/year (11% reduction) or decreasing the TCI from 72 to 57 M\$ (20% reduction). The ROI approaches 15%/year when the lignin price is close to 180 \$/t (30% reduction).

A large plant size is preferred with regard to economies of scale [41]. The effects of the plant size, in the range of 5–100 t/h of Kraft lignin, on the ROI and PBP are shown in Fig. 6. The ROI trend is opposite to that of the PBP, as presented in Eqs. (10) and (11). The plant size of 20 t/h Kraft lignin provides an ROI over 15%/year and a PBP of approximately 5 years.

5 Conclusion

This study presented a conceptual design for vanillin production from Kraft lignin in a 10 t/h plant. Vanillin produced from the alkaline oxidation of lignin was recovered via ultrafiltration, chromatographic separation, and crystallization, where the overall recovery based on the feed lignin was 5.2%.

Alkali regeneration and wastewater treatment were fully taken into account. The energy consumption was reduced via heat integration over the entire plant. The ROI and PBP were 10.1%/year and 8.0 years. The ROI can exceed 15%/year for a plant using 20 t/h Kraft lignin, which makes the vanillin plant economically feasible. The proposed vanillin production plant may be applicable to the pulping processes having the recovery boiler and wastewater treatment unit, saving the capital cost.

Supplementary Information The online version contains supplementary material available at <https://doi.org/10.1007/s13399-020-01212-z>.

Funding This work was supported by the National Research Foundation of Korea (NRF) grant, funded by the Korean Government (MEST and MIST) (grant number: 2020R1F1A1066097, 2020M1A2A207980211, and 2019R1G1A1003364).

Compliance with ethical standards

Conflict of interest The authors declare that they have no conflict of interest.

References

- Cabral Almada C, Kazachenko A, Fongarland P, Da Silva PD, Kuznetsov BN, Djakovitch L (2020) Oxidative depolymerization of lignins for producing aromatics: variation of botanical origin and extraction methods. *Biomass Convers Bior.* <https://doi.org/10.1007/s13399-020-00897-6>
- Wu Z, Hu L, Jiang Y, Wang X, Xu J, Wang Q, Jiang S (2020) Recent advances in the acid-catalyzed conversion of lignin. *Biomass Convers Bior.* <https://doi.org/10.1007/s13399-020-00976-8>
- Mahmood N, Yuan Z, Schmidt J, Charles Xu C (2013) Production of polyols via direct hydrolysis of Kraft lignin: effect of process parameters. *Bioresour Technol* 139:13–20. <https://doi.org/10.1016/j.biortech.2013.03.199>
- Wongtanyawat N, Lusanandana P, Khwanjaisakun N, Kongpana P, Phromprasit J, Simasatitkul L, Amomraksa S, Assabumrungrat S (2018) Comparison of different Kraft lignin-based vanillin production processes. *Comput Chem Eng* 117:159–170. <https://doi.org/10.1016/j.compchemeng.2018.05.020>
- Bajwa DS, Pourhashem G, Ullah AH, Bajwa SG (2019) A concise review of current lignin production, applications, products and their environmental impact. *Ind Crop Prod* 139:111526. <https://doi.org/10.1016/j.indcrop.2019.111526>
- Laurichesse S, Avérous L (2014) Chemical modification of lignins: towards biobased polymers. *Prog Polym Sci* 39(7):1266–1290. <https://doi.org/10.1016/j.progpolymsci.2013.11.004>
- Zhang R, Maltari R, Guo M, Kontro J, Eronen A, Repo T (2020) Facile synthesis of vanillin from fractionated Kraft lignin. *Ind Crop Prod* 145:112095. <https://doi.org/10.1016/j.indcrop.2020.112095>
- Fache M, Boutevin B, Caillol S (2016) Vanillin production from lignin and its use as a renewable chemical. *ACS Sustain Chem Eng* 4(1):35–46. <https://doi.org/10.1021/acssuschemeng.5b01344>
- Sudarsanam P, Duolikun T, Babu PS, Rokhum L, Johan MR (2019) Recent developments in selective catalytic conversion of lignin into aromatics and their derivatives. *Biomass Convers Bior* 10:873–883. <https://doi.org/10.1007/s13399-019-00530-1>

10. Chio C, Sain M, Qin W (2019) Lignin utilization: a review of lignin depolymerization from various aspects. *Renew Sust Energ Rev* 107:232–249. <https://doi.org/10.1016/j.rser.2019.03.008>
11. Araújo JDP, Grande CA, Rodrigues AE (2009) Structured packed bubble column reactor for continuous production of vanillin from Kraft lignin oxidation. *Catal Today* 147:S330–S335. <https://doi.org/10.1016/j.cattod.2009.07.016>
12. Fache M, Boutevin B, Caillol S (2016) Epoxy thermosets from model mixtures of the lignin-to-vanillin process. *Green Chem* 18(3):712–725. <https://doi.org/10.1039/c5gc01070e>
13. Tarabanko VE, Tarabanko N (2017) Catalytic oxidation of lignins into the aromatic aldehydes: general process trends and development prospects. *Int J Mol Sci* 18(11):2421. <https://doi.org/10.3390/ijms18112421>
14. Rodrigues A, Pinto P, Barreiro M, Costa C, Mota I, Fernandes I (2018) An integrated approach for added-value products from lignocellulosic biorefineries: vanillin, syringaldehyde, polyphenols and polyurethane. Springer, Switzerland. <https://doi.org/10.1007/978-3-319-99313-3>
15. Gomes ED, Rodrigues AE (2020) Crystallization of vanillin from kraft lignin oxidation. *Sep Purif Technol* 247:116977. <https://doi.org/10.1016/j.seppur.2020.116977>
16. Khwanjaisakun N, Amornraksa S, Simasatitkul L, Charoensuppanimit P, Assabumrungrat S (2020) Techno-economic analysis of vanillin production from kraft lignin: feasibility study of lignin valorization. *Bioresour Technol* 299:122559. <https://doi.org/10.1016/j.biortech.2019.122559>
17. Lyu G, Yoo CG, Pan X (2018) Alkaline oxidative cracking for effective depolymerization of biorefining lignin to mono-aromatic compounds and organic acids with molecular oxygen. *Biomass Bioenergy* 108:7–14. <https://doi.org/10.1016/j.biombioe.2017.10.046>
18. Pinto PCR, Costa CE, Rodrigues AE (2013) Oxidation of lignin from *Eucalyptus globulus* pulping liquors to produce syringaldehyde and vanillin. *Ind Eng Chem Res* 52(12):4421–4428. <https://doi.org/10.1021/ie303349j>
19. Mathias AL, Rodrigues AE (1995) Production of vanillin by oxidation of pine Kraft lignins with oxygen. *Holzforschung* 49:273–278. <https://doi.org/10.1515/hfsg.1995.49.3.273>
20. EABd S, Zabkova M, Araújo JD, Cateto CA, Barreiro MF, Belgacem MN, Rodrigues AE (2009) An integrated process to produce vanillin and lignin-based polyurethanes from Kraft lignin. *Chem Eng Res Des* 87(9):1276–1292. <https://doi.org/10.1016/j.chemd.2009.05.008>
21. Araújo JDP, Grande CA, Rodrigues AE (2010) Vanillin production from lignin oxidation in a batch reactor. *Chem Eng Res Des* 88(8):1024–1032. <https://doi.org/10.1016/j.chemd.2010.01.021>
22. Jeon W, Choi I-H, Park J-Y, Lee J-S, Hwang K-R (2020) Alkaline wet oxidation of lignin over Cu-Mn mixed oxide catalysts for production of vanillin. *Catal Today* 352:95–103. <https://doi.org/10.1016/j.cattod.2019.12.037>
23. Gomes ED, Rodrigues AE (2020) Recovery of vanillin from kraft lignin depolymerization with water as desorption eluent. *Sep Purif Technol* 239:116551. <https://doi.org/10.1016/j.seppur.2020.116551>
24. Gomes ED, Mota MI, Rodrigues AE (2018) Fractionation of acids, ketones and aldehydes from alkaline lignin oxidation solution with SP700 resin. *Sep Purif Technol* 194:256–264. <https://doi.org/10.1016/j.seppur.2017.11.050>
25. Partenheimer W (2009) The aerobic oxidative cleavage of lignin to produce hydroxyaromatic benzaldehydes and carboxylic acids via metal/bromide catalysts in acetic acid/water mixtures. *Adv Synth Catal* 351(3):456–466. <https://doi.org/10.1002/adsc.200800614>
26. Voitl T, Rohr PRv (2010) Demonstration of a process for the conversion of Kraft lignin into vanillin and methyl vanillate by acidic oxidation in aqueous methanol. *Ind Eng Chem Res* 49(2):520–525. <https://doi.org/10.1021/ie901293p>
27. Werhan H (2013) A process for the complete valorization of lignin into aromatic chemicals based on acidic oxidation. PhD thesis, ETH Zürich, Zürich
28. Zabkova M, da Silva EAB, Rodrigues AE (2007) Recovery of vanillin from lignin/vanillin mixture by using tubular ceramic ultrafiltration membranes. *J Membr Sci* 301(1):221–237. <https://doi.org/10.1016/j.memsci.2007.06.025>
29. Abdelaziz OY, Li K, Tunã P, Hulteberg CP (2018) Continuous catalytic depolymerisation and conversion of industrial Kraft lignin into low-molecular-weight aromatics. *Biomass Convers Bior* 8(2):455–470. <https://doi.org/10.1007/s13399-017-0294-2>
30. Do TX, Y-i L, Yeo H, Lee U-d, Y-t C, J-h S (2014) Techno-economic analysis of power plant via circulating fluidized-bed gasification from woodchips. *Energy* 70:547–560. <https://doi.org/10.1016/j.energy.2014.04.048>
31. Arkell A, Olsson J, Wallberg O (2014) Process performance in lignin separation from softwood black liquor by membrane filtration. *Chem Eng Res Des* 92(9):1792–1800. <https://doi.org/10.1016/j.chemd.2013.12.018>
32. Gomes ED, Rodrigues AE (2019) Lignin biorefinery: separation of vanillin, vanillic acid and acetovanillone by adsorption. *Sep Purif Technol* 216:92–101. <https://doi.org/10.1016/j.seppur.2019.01.071>
33. Cartwright LC (1953) Vanilla-like synthetics, solubility, and volatility of propenyl guaethyl, bourbonal, vanillin, and coumarin. *J Agric Food Chem* 1(4):312–314. <https://doi.org/10.1021/jf60004a006>
34. Humbird D, Davis R, Tao L, Kinchin C, Hsu D, Aden A, Schoen P, Lukas J, Olthof B, Worley M, Sexton D, Dudgeon D (2011) Process design and economics for biochemical conversion of lignocellulosic biomass to ethanol: dilute-acid pretreatment and enzymatic hydrolysis of corn stover. NREL, Golden
35. Kim S, Lim Y-I, Lee D, Seo MW, Mun T-Y, Lee J-G (2020) Effects of flue gas recirculation on energy, exergy, environment, and economics in oxy-coal circulating fluidized-bed power plants with CO₂ capture. *Int J Energy Res* in press. <https://doi.org/10.1002/er.6205>
36. Sanchez DR (2000) Reausticizing-principles and practice: kraft recovery short course. TAPPI Press, Orlando
37. Lundqvist P (2009) Mass and energy balances over the lime kiln in a Kraft pulp mill. Master thesis, Uppsala University, Uppsala
38. Nielsen S, Christensen SWS, Thorsen R, Imegaard B Comparison of heat pump design and performance for modern refrigerants. In: 13th IIR-Gustav Lorentzen Conference on Natural Refrigerants, Valencia, Spain, 2018. International Institute of Refrigeration, pp 307–314. <https://doi.org/10.18462/iir.gl.2018.1149>
39. Rangaiah GP (2016) Chemical process retrofitting and revamping: techniques and applications, First edn. John Wiley & Sons, New York
40. Do TX, Y-i L (2016) Techno-economic comparison of three energy conversion pathways from empty fruit bunches. *Renew Energy* 90:307–318. <https://doi.org/10.1016/j.renene.2016.01.030>
41. Do TX, Lim YI, Jang S, Chung HJ (2015) Hierarchical economic potential approach for techno-economic evaluation of bioethanol production from palm empty fruit bunches. *Bioresour Technol* 189:224–235. <https://doi.org/10.1016/j.biortech.2015.04.020>
42. Kemp IC (2006) Pinch analysis and process integration: a user guide on process integration for the efficient use of energy, Second edn. Butterworth-Heinemann, Oxford
43. Do TX, Y-i L, Cho H, Shim J, Yoo J, Rho K, Choi S-G, Park C, Park B-Y (2018) Techno-economic analysis of fry-drying and torrefaction plant for bio-solid fuel production. *Renew Energy* 119:45–53. <https://doi.org/10.1016/j.renene.2017.11.085>
44. Vu TT, Lim Y-I, Song D, Mun T-Y, Moon J-H, Sun D, Hwang Y-T, Lee J-G, Park YC (2020) Techno-economic analysis of ultra-supercritical power plants using air- and oxy-combustion

- circulating fluidized bed with and without CO₂ capture. *Energy* 194:116855. <https://doi.org/10.1016/j.energy.2019.116855>
45. Davis R, Grundl N, Tao L, Bidy MJ, Tan ECD, Beckham GT, Humbird D, Thompson DN, Roni MS (2018) Process design and economics for the conversion of lignocellulosic biomass to hydrocarbon fuels and coproducts: 2018 biochemical design case update. NREL, Golden
 46. Davis R, Tao L, Scarlata C, Tan ECD, Ross J, Lukas J, Sexton D (2015) Process design and economics for the conversion of lignocellulosic biomass to hydrocarbons dilute-acid and enzymatic deconstruction of biomass to sugars and catalytic conversion of sugars to hydrocarbons. NREL, Golden
 47. Couper JR, Penney WR, Fair JR (2012) Chemical process equipment: selection and design, Third edn. Butterworth-Heinemann, Oxford
 48. Do TX, Mujahid R, Lim HS, Kim J-K, Lim Y-I, Kim J (2020) Techno-economic analysis of bio heavy-oil production from sewage sludge using supercritical and subcritical water. *Renew Energy* 151:30–42. <https://doi.org/10.1016/j.renene.2019.10.138>
 49. Otromke M, Shuttleworth PS, Sauer J, White RJ (2019) Hydrothermal base catalysed treatment of Kraft lignin-time dependent analysis and a techno-economic evaluation for carbon fibre applications. *Bioresour Technol Rep* 6:241–250. <https://doi.org/10.1016/j.biteb.2019.03.008>

Publisher's Note Springer Nature remains neutral with regard to jurisdictional claims in published maps and institutional affiliations.